View metadata, citation and similar papers at core.ac.uk

brought to you by CORE

provided by HAL Clermont Université

Measurement of the tau lepton lifetime with the three-dimensional impact parameter method.

R. Barate, D. Buskulic, D. Decamp, P. Ghez, C. Goy, J P. Lees, A. Lucotte, M N. Minard, J Y. Nief, P. Odier, et al.

To cite this version:

R. Barate, D. Buskulic, D. Decamp, P. Ghez, C. Goy, et al.. Measurement of the tau lepton lifetime with the three-dimensional impact parameter method.. Zeitschrift für Physik C Particles and Fields, Springer Verlag, 1997, 74, pp.387-398. <in2p3-00010762>

HAL Id: in2p3-00010762

http://hal.in2p3.fr/in2p3-00010762

Submitted on 18 Jan 1999

HAL is a multi-disciplinary open access archive for the deposit and dissemination of scientific research documents, whether they are published or not. The documents may come from teaching and research institutions in France or abroad, or from public or private research centers.

L'archive ouverte pluridisciplinaire **HAL**, est destinée au dépôt et à la diffusion de documents scientifiques de niveau recherche, publiés ou non, émanant des établissements d'enseignement et de recherche français ou étrangers, des laboratoires publics ou privés.

EUROPEAN ORGANIZATION FOR NUCLEAR RESEARCH

CERN–PPE/97–016
6 February 1997

Measurement of the τ Lepton Lifetime with the Three-dimensional Impact Parameter Method

Abstract

A new method is presented for the measurement of the mean τ lepton lifetime using events in which τ's are pair-produced and both τ's decay to hadrons and ν_τ. Based on the correlation between the two τ's produced at a symmetric e^+e^- collider, the 3DIP method relies on the three-dimensional information from a double-sided vertex detector and on kinematic constraints for the precise measurement of the τ decay angles. Using the data collected from 1992 to 1994 with the ALEPH detector at LEP, a τ lifetime of $288.0 \pm 3.1 \pm 1.3$ fs is obtained from the sample in which both τ's decay to one charged track, and $292.8 \pm 5.6 \pm 3.0$ fs from the sample in which one τ decays to one prong and the other to three prongs. The results show small statistical correlations with those derived from other methods. When combined with the previously published ALEPH measurements, the resulting τ lifetime is $291.2 \pm 2.0 \pm 1.2$ fs.

The ALEPH Collaboration*

(Submitted to Z. Phys. C)

*See the following pages for the list of authors.

The ALEPH Collaboration

R. Barate, D. Buskulic, D. Decamp, P. Ghez, C. Goy, J.-P. Lees, A. Lucotte, M.-N. Minard, J.-Y. Nief, B. Pietrzyk

Laboratoire de Physique des Particules (LAPP), IN^{2}P^3-CNRS, 74019 Annecy-le-Vieux Cedex, France

M.P. Casado, M. Chmeissani, P. Comas, J.M. Crespo, M. Delfino, E. Fernandez, M. Fernandez-Bosman, Ll. Garrido,[15] A. Juste, M. Martinez, R. Miquel, Ll.M. Mir, S. Orteu, C. Padilla, I.C. Park, A. Pascual, J.A. Perlas, I. Riu, F. Sanchez, F. Teubert

Institut de Fisica d'Altes Energies, Universitat Autonoma de Barcelona, 08193 Bellaterra (Barcelona), Spain[7]

A. Colaleo, D. Creanza, M. de Palma, G. Gelao, G. Iaselli, G. Maggi, M. Maggi, N. Marinelli, S. Nuzzo, A. Ranieri, G. Raso, F. Ruggieri, G. Selvaggi, L. Silvestris, P. Tempesta, A. Tricomi,[3] G. Zito

Dipartimento di Fisica, INFN Sezione di Bari, 70126 Bari, Italy

X. Huang, J. Lin, Q. Ouyang, T. Wang, Y. Xie, R. Xu, S. Xue, J. Zhang, L. Zhang, W. Zhao

Institute of High-Energy Physics, Academia Sinica, Beijing, The People's Republic of China[8]

D. Abbaneo, R. Alemany, U. Becker, A.O. Bazarko,[20] P. Bright-Thomas, M. Cattaneo, F. Cerutti, H. Drevermann, R.W. Forty, M. Frank, R. Hagelberg, J. Harvey, P. Janot, B. Jost, E. Kneringer, J. Knobloch, I. Lehraus, G. Lutters, P. Mato, A. Minten, L. Moneta, A. Pacheco, J.-F. Pusztaszeri, F. Ranjard, P. Rensing,[12] G. Rizzo, L. Rolandi, D. Schlatter, M. Schmitt, O. Schneider, W. Tejessy, I.R. Tomalin, H. Wachsmuth, A. Wagner

European Laboratory for Particle Physics (CERN), 1211 Geneva 23, Switzerland

Z. Ajaltouni, A. Barrès, C. Boyer, A. Falvard, C. Ferdi, P. Gay, C . Guicheney, P. Henrard, J. Jousset, B. Michel, S. Monteil, J-C. Montret, D. Pallin, P. Perret, F. Podlyski, J. Proriol, P. Rosnet, J.-M. Rossignol

Laboratoire de Physique Corpusculaire, Université Blaise Pascal, IN^{2}P^3-CNRS, Clermont-Ferrand, 63177 Aubière, France

T. Fearnley, J.B. Hansen, J.D. Hansen, J.R. Hansen, P.H. Hansen, B.S. Nilsson, B. Rensch, A. Wäänänen

Niels Bohr Institute, 2100 Copenhagen, Denmark[9]

G. Daskalakis, A. Kyriakis, C. Markou, E. Simopoulou, I. Siotis, A. Vayaki

Nuclear Research Center Demokritos (NRCD), Athens, Greece

A. Blondel, G. Bonneaud, J.C. Brient, P. Bourdon, A. Rougé, M. Rumpf, A. Valassi,[6] M. Verderi, H. Videau

Laboratoire de Physique Nucléaire et des Hautes Energies, Ecole Polytechnique, IN^{2}P^3-CNRS, 91128 Palaiseau Cedex, France

D.J. Candlin, M.I. Parsons

Department of Physics, University of Edinburgh, Edinburgh EH9 3JZ, United Kingdom[10]

E. Focardi, G. Parrini, K. Zachariadou

Dipartimento di Fisica, Università di Firenze, INFN Sezione di Firenze, 50125 Firenze, Italy

M. Corden, C. Georgiopoulos, D.E. Jaffe

Supercomputer Computations Research Institute, Florida State University, Tallahassee, FL 32306-4052, USA [13,14]

A. Antonelli, G. Bencivenni, G. Bologna,[4] F. Bossi, P. Campana, G. Capon, D. Casper, V. Chiarella, G. Felici, P. Laurelli, G. Mannocchi,[5] F. Murtas, G.P. Murtas, L. Passalacqua, M. Pepe-Altarelli

Laboratori Nazionali dell'INFN (LNF-INFN), 00044 Frascati, Italy

L. Curtis, S.J. Dorris, A.W. Halley, I.G. Knowles, J.G. Lynch, V. O'Shea, C. Raine, J.M. Scarr, K. Smith, P. Teixeira-Dias, A.S. Thompson, E. Thomson, F. Thomson, R.M. Turnbull

Department of Physics and Astronomy, University of Glasgow, Glasgow G12 8QQ,United Kingdom[10]

C. Geweniger, G. Graefe, P. Hanke, G. Hansper, V. Hepp, E.E. Kluge, A. Putzer, M. Schmidt, J. Sommer, K. Tittel, S. Werner, M. Wunsch

Institut für Hochenergiephysik, Universität Heidelberg, 69120 Heidelberg, Fed. Rep. of Germany[16]

R. Beuselinck, D.M. Binnie, W. Cameron, P.J. Dornan, M. Girone, S. Goodsir, E.B. Martin, A. Moutoussi, J. Nash, J.K. Sedgbeer, A.M. Stacey, M.D. Williams

Department of Physics, Imperial College, London SW7 2BZ, United Kingdom[10]

G. Dissertori, P. Girtler, D. Kuhn, G. Rudolph

Institut für Experimentalphysik, Universität Innsbruck, 6020 Innsbruck, Austria[18]

A.P. Betteridge, C.K. Bowdery, P. Colrain, G. Crawford, A.J. Finch, F. Foster, G. Hughes, T. Sloan, M.I. Williams

Department of Physics, University of Lancaster, Lancaster LA1 4YB, United Kingdom[10]

A. Galla, I. Giehl, A.M. Greene, C. Hoffmann, K. Jakobs, K. Kleinknecht, G. Quast, B. Renk, E. Rohne, H.-G. Sander, P. van Gemmeren, C. Zeitnitz

Institut für Physik, Universität Mainz, 55099 Mainz, Fed. Rep. of Germany[16]

J.J. Aubert, C. Benchouk, A. Bonissent, G. Bujosa, D. Calvet, J. Carr, P. Coyle, C. Diaconu, F. Etienne, N. Konstantinidis, O. Leroy, F. Motsch, P. Payre, D. Rousseau, M. Talby, A. Sadouki, M. Thulasidas, K. Trabelsi

Centre de Physique des Particules, Faculté des Sciences de Luminy, IN^{2}P^3-CNRS, 13288 Marseille, France

M. Aleppo, F. Ragusa[2]

Dipartimento di Fisica, Università di Milano e INFN Sezione di Milano, 20133 Milano, Italy

R. Berlich, W. Blum, V. Büscher, H. Dietl, F. Dydak,[2] G. Ganis, C. Gotzhein, H. Kroha, G. Lütjens, G. Lutz, W. Männer, H.-G. Moser, R. Richter, A. Rosado-Schlosser, S. Schael, R. Settles, H. Seywerd, R. St. Denis, H. Stenzel, W. Wiedenmann, G. Wolf

Max-Planck-Institut für Physik, Werner-Heisenberg-Institut, 80805 München, Fed. Rep. of Germany[16]

J. Boucrot, O. Callot,[2] S. Chen, Y. Choi,[21] A. Cordier, M. Davier, L. Duflot, J.-F. Grivaz, Ph. Heusse, A. Höcker, A. Jacholkowska, M. Jacquet, D.W. Kim,[24] F. Le Diberder, J. Lefrançois, A.-M. Lutz, I. Nikolic, M.-H. Schune, S. Simion, E. Tournefier, J.-J. Veillet, I. Videau, D. Zerwas

Laboratoire de l'Accélérateur Linéaire, Université de Paris-Sud, IN^{2}P^3-CNRS, 91405 Orsay Cedex, France

P. Azzurri, G. Bagliesi, G. Batignani, S. Bettarini, C. Bozzi, G. Calderini, M. Carpinelli, M.A. Ciocci, V. Ciulli, R. Dell'Orso, R. Fantechi, I. Ferrante, L. Foà,[1] F. Forti, A. Giassi, M.A. Giorgi, A. Gregorio, F. Ligabue, A. Lusiani, P.S. Marrocchesi, A. Messineo, F. Palla, G. Sanguinetti, A. Sciabà, P. Spagnolo, J. Steinberger, R. Tenchini, G. Tonelli,[19] C. Vannini, A. Venturi, P.G. Verdini

Dipartimento di Fisica dell'Università, INFN Sezione di Pisa, e Scuola Normale Superiore, 56010 Pisa, Italy

G.A. Blair, L.M. Bryant, J.T. Chambers, Y. Gao, M.G. Green, T. Medcalf, P. Perrodo, J.A. Strong, J.H. von Wimmersperg-Toeller

Department of Physics, Royal Holloway & Bedford New College, University of London, Surrey TW20 OEX, United Kingdom[10]

D.R. Botterill, R.W. Clifft, T.R. Edgecock, S. Haywood, P. Maley, P.R. Norton, J.C. Thompson, A.E. Wright

Particle Physics Dept., Rutherford Appleton Laboratory, Chilton, Didcot, Oxon OX11 OQX, United Kingdom[10]

B. Bloch-Devaux, P. Colas, S. Emery, W. Kozanecki, E. Lançon, M.C. Lemaire, E. Locci, P. Perez, J. Rander, J.-F. Renardy, A. Roussarie, J.-P. Schuller, J. Schwindling, A. Trabelsi, B. Vallage

CEA, DAPNIA/Service de Physique des Particules, CE-Saclay, 91191 Gif-sur-Yvette Cedex, France[17]

S.N. Black, J.H. Dann, R.P. Johnson, H.Y. Kim, A.M. Litke, M.A. McNeil, G. Taylor

Institute for Particle Physics, University of California at Santa Cruz, Santa Cruz, CA 95064, USA[22]

C.N. Booth, R. Boswell, C.A.J. Brew, S. Cartwright, F. Combley, M.S. Kelly, M. Lehto, W.M. Newton, J. Reeve, L.F. Thompson

Department of Physics, University of Sheffield, Sheffield S3 7RH, United Kingdom[10]

A. Böhrer, S. Brandt, G. Cowan, C. Grupen, P. Saraiva, L. Smolik, F. Stephan

Fachbereich Physik, Universität Siegen, 57068 Siegen, Fed. Rep. of Germany[16]

M. Apollonio, L. Bosisio, R. Della Marina, G. Giannini, B. Gobbo, G. Musolino

Dipartimento di Fisica, Università di Trieste e INFN Sezione di Trieste, 34127 Trieste, Italy

J. Rothberg, S. Wasserbaech

Experimental Elementary Particle Physics, University of Washington, WA 98195 Seattle, U.S.A.

S.R. Armstrong, E. Charles, P. Elmer, D.P.S. Ferguson, Y.S. Gao,[23] S. González, T.C. Greening, O.J. Hayes, H. Hu, S. Jin, P.A. McNamara III, J.M. Nachtman, J. Nielsen, W. Orejudos, Y.B. Pan, Y. Saadi, I.J. Scott, J. Walsh, Sau Lan Wu, X. Wu, J.M. Yamartino, G. Zobernig

Department of Physics, University of Wisconsin, Madison, WI 53706, USA[11]

---

[1]Now at CERN, 1211 Geneva 23, Switzerland.
[2]Also at CERN, 1211 Geneva 23, Switzerland.
[3]Also at Dipartimento di Fisica, INFN, Sezione di Catania, Catania, Italy.
[4]Also Istituto di Fisica Generale, Università di Torino, Torino, Italy.
[5]Also Istituto di Cosmo-Geofisica del C.N.R., Torino, Italy.
[6]Supported by the Commission of the European Communities, contract ERBCHBICT941234.
[7]Supported by CICYT, Spain.
[8]Supported by the National Science Foundation of China.
[9]Supported by the Danish Natural Science Research Council.
[10]Supported by the UK Particle Physics and Astronomy Research Council.
[11]Supported by the US Department of Energy, grant DE-FG0295-ER40896.
[12]Now at Dragon Systems, Newton, MA 02160, U.S.A.
[13]Supported by the US Department of Energy, contract DE-FG05-92ER40742.
[14]Supported by the US Department of Energy, contract DE-FC05-85ER250000.
[15]Permanent address: Universitat de Barcelona, 08208 Barcelona, Spain.
[16]Supported by the Bundesministerium für Bildung, Wissenschaft, Forschung und Technologie, Fed. Rep. of Germany.
[17]Supported by the Direction des Sciences de la Matière, C.E.A.
[18]Supported by Fonds zur Förderung der wissenschaftlichen Forschung, Austria.
[19]Also at Istituto di Matematica e Fisica, Università di Sassari, Sassari, Italy.
[20]Now at Princeton University, Princeton, NJ 08544, U.S.A.
[21]Permanent address: Sung Kyun Kwan University, Suwon, Korea.
[22]Supported by the US Department of Energy, grant DE-FG03-92ER40689.
[23]Now at Harvard University, Cambridge, MA 02138, U.S.A.
[24]Permanent address: Kangnung National University, Kangnung, Korea.

1 Introduction

Since the early measurements of τ lepton lifetime, several methods have been designed to increase the precision [1]. The decay length (DL) method, based on the measurement of the decay vertex in the three-prong τ decays, has a high sensitivity but is statistically limited due to the small branching ratios of three-prong channels and to vertexing efficiency. Other methods have been developed to use one-prong decays of the τ. All are based on the measurement of the impact parameter (IP) of the charged daughter track with respect to the τ production point, in the plane transverse to the beams. The simple IP method depends on the knowledge of the τ direction from the thrust or sphericity axis of the decay products to sign the impact parameter, and the measurement is smeared by the beam size. Other methods — impact parameter difference (IPD) [2], impact parameter sum (IPS [3], momentum weighted IPS [4], miss distance [5]) — can alleviate one of the uncertainties (τ direction or τ production point) but not both; in some cases, they are furthermore very sensitive to the assumed detector resolution.

The new approach presented here is designed to overcome these limitations. Restricted to events in which both τ's undergo hadronic decays, the procedure applies to one-prong as well as three-prong decays. The decay angles are derived from two-body decay kinematics and the method is independent of the uncertainty on the τ direction. The uncertainty on the τ production point is minimised by measuring a quantity related to the miss distance in space between the τ decay tracks. As a three-dimensional method, it exploits the high precision in r-ϕ and z presently achieved with vertex detectors.

The method is applied to a sample of 105000 τ pair events selected in the data taken from 1992 to 1994 with the ALEPH detector at the LEP collider.

2 Method

2.1 τ decay topology and kinematics

At LEP, the τ flight distance in $e^+e^- \to \tau^+\tau^-$ events is of the order of 2 mm. The τ decay point can be measured only in three-prong decays (15% of τ decays) with a typical longitudinal error of 750 μm and transverse error of 25 μm. The τ production point is known only to the precision of the size of the beam luminous region, up to $\sim$150 μm transverse to the beams in the LEP plane and 7 mm along the beams. Because of missing neutrinos in the final state, the τ direction cannot be directly deduced from its measured decay products and the classical approximation of the τ axis by the thrust or sphericity axis of the event has a typical error of 30 mrad. Therefore, neither the τ path nor the flight direction can be measured directly with accuracy. However, most of the information can be recovered by using geometrical relations and kinematic constraints.

As shown in Fig. 1, vector relations between the τ direction $\hat{\tau}$, the τ decay length ℓ, and the direction of the decay track $\hat{c}$, can be inferred from simple geometrical considerations in the three-dimensional space. Let C_0 be the point on the extrapolated charged daughter at the closest approach to the beam axis. C_0 is defined by the measured parameters of the track, ϕ_0, d_0 and z_0, respectively its azimuth, radial distance and coordinate along the beam at the point of closest approach. In the case of three-prong decays, a sum track, as

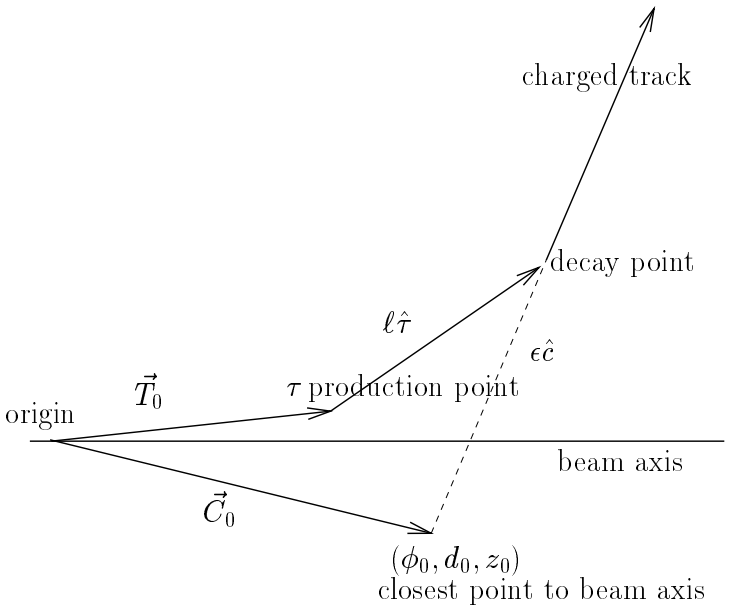

Figure 1: Not-to-scale view of a τ decay to one charged track. The decay angle is exaggerated for the sake of the drawing.

defined from the secondary vertex and the vector sum of charged daughter momenta, is used. Elementary geometry leads to the following equation:

$$\vec{T}_0 + \ell\hat{\tau} = \vec{C}_0 + \epsilon\hat{c} \tag{1}$$

where T_0 is the τ production point with respect to the coordinate origin, chosen at the centre of the beam luminous region. Under the assumption that the τ originates from the beam axis, this equation, projected onto the r-ϕ plane, leads to the classical relation between impact parameter and decay length, $d_0 = \ell \sin\theta \sin\psi_{xy}$, where θ is the τ polar angle and ψ_{xy} is the azimuthal difference between τ and charged track directions. The projection onto the transverse plane has until now been the basis of all methods using impact parameters. This choice resulted from the poor accuracy of z measurements from the earlier tracking systems, from the large longitudinal size of the beam luminous region and from the concern for minimising the projected acollinearity of the τ's in methods using τ pairs.

When both hemispheres are considered simultaneously, the τ pair production point cancels out in the difference of Eq. (1) as applied to τ^+ and τ^-. This is the basis of impact parameter sum methods, where the effect of the beam size is strictly null when the daughter tracks are back to back in the transverse plane. However the measurement is impeded by the τ direction uncertainty in the ψ_{xy} angle determination. Conversely, the τ

direction uncertainty cancels out in the difference of ψ_{xy} angles used in the IPD method, again under the assumption that the τ^+ and τ^- are back to back, but the transverse beam size enters the τ production point uncertainty twice.

The present approach is designed to be simultaneously insensitive to the beam size and to the τ direction measurement. Like IPD and IPS, the method assumes that the τ's are produced back to back. To cancel the effects of the beam size, it measures, as IPS methods do, the distance between the decay tracks at their points of closest approach to the beam axis. The novel procedure is to depart from the conventional projection onto the r-ϕ plane and to rely on kinematics to define an optimum projecting direction in three-dimensional space.

According to two-body decay kinematics for τ decays to hadrons and neutrino, $\tau \to \nu_\tau h$, the τ direction is constrained to lie on a cone around the measured direction of the hadronic system, with opening angle ψ:

$$\cos\psi = \frac{2E_\tau E_h - m_\tau^2 - m_h^2}{2P_\tau P_h}, \tag{2}$$

where E, P, m are the energy, momentum and mass, respectively. The τ mass is set to $m_\tau = 1.777\,\mathrm{GeV}/c^2$ [6] and the τ energy is taken equal to the beam energy, ignoring radiative corrections; $(E_h, \vec{P}_h)$ is the measured four-momentum of the hadronic final state h. The latter may be a complex object (a_1, ρ, ...) of measured mass m_h; its four-momentum is then measured as the sum of the four-momenta of its charged and neutral daughters.

When considering events in which τ's are pair-produced in a back-to-back topology and both τ's decay to hadrons (42% of all τ pairs), the common direction $\hat{\tau} \equiv \hat{\tau}^+ = -\hat{\tau}^-$ lies along one of the intersections of the two cones [7] (Fig. 2). Considering not only kinematics but also the τ flight path in space, that twofold ambiguity can theoretically be solved when both τ's decay to purely charged modes (without π^0's). However, with the present accuracy of vertex detectors, the ambiguity often cannot be resolved in practice. Furthermore, the lack of precise information on the spatial origin of neutrals prevents a straightforward generalisation of the procedure to τ decays including π^0's and the ambiguity remains in those cases [8]. Still, from kinematics alone, three mutually orthogonal vectors can be unambiguously and precisely measured: $\vec{A}_h$ and $\vec{h}_\perp$, respectively the internal and external bisectors of the two τ vector solutions, and $\vec{H}$, the normal to the ambiguity plane (Fig. 2). Their definitions rely only on the measurement of the hadron directions, $\hat{h}^+$ and $\hat{h}^-$, and the τ decay angles $\psi^\pm$ defined by Eq. (2).

The normal vector $\vec{H}$, defined as

$$\vec{H} \equiv \hat{h}^+ \cos\psi^- + \hat{h}^- \cos\psi^+,$$

is of special importance since in the absence of detector-induced distortions and ignoring radiative corrections, it defines a direction strictly normal to the true τ direction.

The orthogonality, defined by $\pm\hat{\tau}^\pm \cdot \hat{H}$, of the reconstructed $\vec{H}$ with the true $\tau^\pm$ directions, is shown in Fig. 3 for $e^+e^- \to \tau^+\tau^-$ events simulated in the ALEPH detector at LEP. While the rms of the orthogonality angle distribution amounts to 35 mrad, the core is well fitted with a 1 mrad wide Gaussian function. Tails extending beyond 20 mrad amount to 14.2% of the events. Part of the tails are caused by a bad measurement of

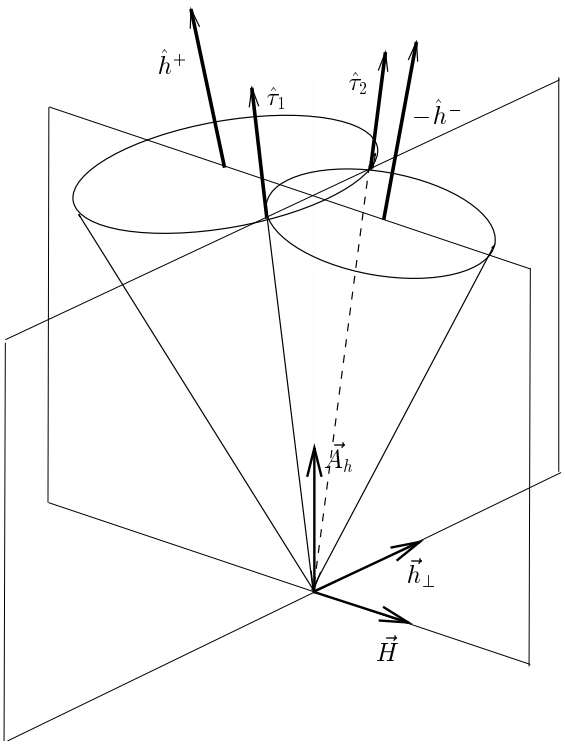

Figure 2: Momentum space representation of the two kinematically allowed τ axis solutions, τ_1 and τ_2, defining the ambiguity plane. The three vectors $\vec{A}_h$, $\vec{h}_\perp$ and $\vec{H}$ are mutually orthogonal. The ambiguity plane coincides with the $h_\perp$-A_h plane and the two hadrons, $\vec{h}^+$ and $\vec{h}^-$, lie in the A_h-H plane.

the hadronic final states, affecting the hadron directions $\hat{h}^\pm$ and $\cos\psi^\pm$; the rest ($\sim$40% of the tails) is due to hard radiation in the initial or final state, affecting $\cos\psi^\pm$ through E_τ, P_τ and/or inducing a large acollinearity between the two τ's. Unlike the conventional methods working in the r-ϕ projection, which are only sensitive to final state radiation effects, the present method might be affected by initial state radiation as well. To reduce the effect, the events suspected to populate the tails of the orthogonality plot are vetoed as explained below (Sect. 3.3.2).

The choice of $\vec{H}$ as the projecting direction is the driving idea of the new method. It is optimal as it is free from the τ direction ambiguity and, compared to the projection along $\vec{A}_h$, it maximises the projected distance between the decay tracks.

2.2 Three-dimensional Impact Parameter relation

In Eq. (1), the distance ϵ between the point of closest approach C_0 and the decay vertex is an unknown quantity. However an approximation of ϵ within 0.1% on average is given by the decay length ℓ itself, due to the transverse beam size and the decay angle being both small (Fig. 1): at LEP energies, the latter does not exceed 170 mrad even if the momentum

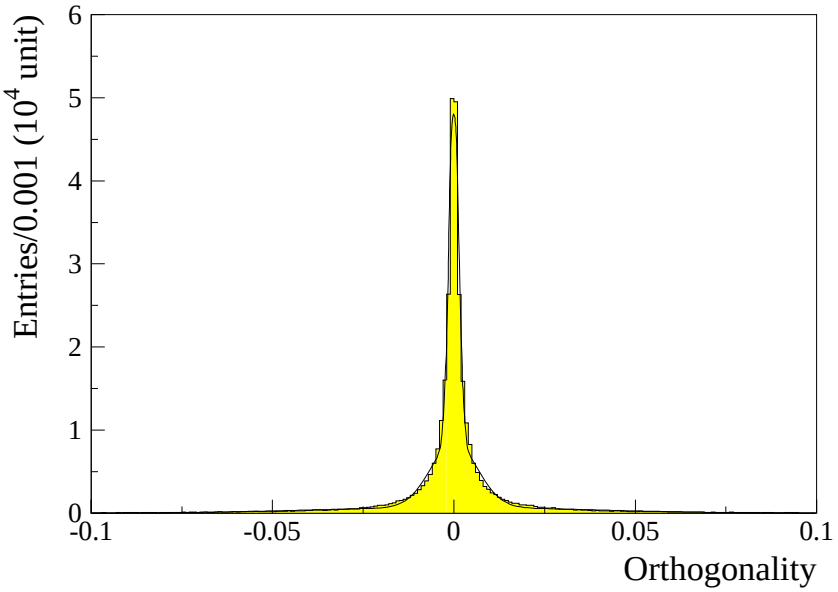

Figure 3: Orthogonality between the reconstructed $\hat{H}$ and the generated τ directions $\hat{\tau}^{\pm}$ in Monte Carlo (see text). Each τ pair event enters the plot twice, with one entry per τ vector. The superimposed curve is a sum of three Gaussian distributions of widths 0.001, 0.006 and 0.034, respectively.

of the hadron is as low as 2 GeV/c. Considering both hemispheres and assuming the τ's to be back to back, $\hat{\tau} \equiv \hat{\tau}^{+} = -\hat{\tau}^{-}$, the difference of Eq. (1) applied to τ^{+} and τ^{-} then becomes

$$\ell^{+}\hat{\tau}^{+} - \ell^{-}\hat{\tau}^{-} \simeq (\ell^{+} + \ell^{-})\hat{\tau} \simeq \delta\vec{C}_0 + \ell^{+}\hat{c}^{+} - \ell^{-}\hat{c}^{-} \tag{3}$$

where $\delta\vec{C}_0 \equiv \vec{C}_0^{+} - \vec{C}_0^{-}$ is the distance between the charged decay tracks at their points of closest approach to the beam.

When projecting along the optimum direction $\vec{H}$, the left-hand term vanishes, due to the orthogonality with the true τ direction. This leads to the basic three-dimensional impact parameter (3DIP) relation

$$\delta \simeq \ell^{+}\alpha^{+} + \ell^{-}\alpha^{-} \tag{4}$$

where $\delta \equiv -\delta\vec{C}_0 \cdot \hat{H}$ and $\alpha^{\pm} \equiv \pm\hat{c}^{\pm} \cdot \hat{H}$.

Equation (4) is formally identical to the IPS equation [3]: ignoring the measurement errors, the expected δ distribution is the algebraic sum of two exponential functions, with slopes inversely proportional to the average τ decay length $\lambda = \gamma\beta c\tau_\tau$. The combination depends on the relative signs and magnitudes of $\alpha^{\pm}$. The measurement of the lifetime is performed through an event-by-event maximum likelihood method similar to that used in the ALEPH IPS analysis [3], with the lifetime τ_τ as a free parameter, the projections along $\vec{H}$ of the track distance δ and track directions $\alpha^{\pm}$ as measured quantities, and Eq. (4) as the constraining relation.

To visualise the similarities between the IPS and 3DIP methods, one can expand δ,

noticing that the charged tracks $\hat{c}^+$ and $\hat{c}^-$ have almost back-to-back azimuths $\phi^{\pm}$:

$$\begin{aligned} \delta &\equiv -\delta\vec{C}_0 \cdot \hat{H} \\ &\sim (d_0^+ + d_0^-)(H_x \sin\bar{\phi} - H_y \cos\bar{\phi}) + (z_0^+ - z_0^-)H_z \end{aligned} \tag{5}$$

with $\bar{\phi} \equiv (\phi^+ + \phi^- \pm \pi)/2$.

While IPS is based on the track miss distance projected to the r-ϕ plane, measured by $d_0^+ + d_0^-$ according to the d_0 sign convention, 3DIP is based on the track miss distance in space, measured by $d_0^+ + d_0^-$ in the transverse plane and $z_0^+ - z_0^-$ along the beams. The 3DIP method can therefore be regarded as an IPS method generalised to the three-dimensional space.

However, the 3DIP and IPS methods differ basically in the angular uncertainties affecting the relationship between δ and the decay angles. Since the undetected neutrinos impede the reconstruction of the τ direction, the r-ϕ projections of the τ decay angles are determined in IPS with an uncertainty of $\sim$20 mrad, which is comparable to the size of the angles themselves. As a consequence, the decay angle error distribution must then be numerically modelled by using simulated events. In the 3DIP method, the choice of $\hat{H}$ as the projecting direction eliminates the uncertainty due to undetected neutrinos and the only errors to be considered in the likelihood function are tracking errors. The only smearing due to the projecting direction comes from its non-orthogonality with the τ direction when the term $(\ell^+\hat{\tau}^+ - \ell^-\hat{\tau}^-) \cdot \hat{H}$ does not actually vanish due to hadron mismeasurement or radiative effects (see Sect. 4.2). Given the average values of decay lengths at LEP energies and the 1 mrad wide core of the orthogonality plot (Fig. 3), the neglected term $(\ell^+\hat{\tau}^+ - \ell^-\hat{\tau}^-) \cdot \hat{H}$ would naively be interpreted as an additional Gaussian error of 4 μm on δ, to be compared to a typical tracking error of 50 μm. However, because that term is directly proportional to the decay length sum, and because of the correlation between $\hat{\tau} \cdot \hat{H}$ and the measured $\alpha^{\pm}$ angles, a systematic bias of a few percent is induced on the lifetime measurement. This is corrected by means of a Monte Carlo simulation as explained in Sect. 4.2.

3 Experimental setup and data selection

3.1 The ALEPH detector

The ALEPH detector is described in detail in references [9] and [10] and only a brief description is given here. The 3DIP method depends on the performance of all major subdetectors, in terms of spatial resolution, energy measurement and particle identification.

Three tracking devices provide three-dimensional information on charged particle trajectories: a large time projection chamber (TPC), a conventional drift chamber (ITC) and a high resolution vertex detector (VDET). The VDET [11] consists of two layers of double-sided silicon wafers. The inner layer, at an average radius of 6.5 cm from the beam axis, covers 85% of the solid angle; the outer layer, at a radius of 11.3 cm, covers 69% of the solid angle. Each layer provides r-ϕ and z measurements. The spatial resolution is 12 μm for r-ϕ coordinates and varies from 12 μm to 22 μm for z coordinates,

depending on the polar angle. The ITC is made of eight concentric axial wire layers, 2 m long, and extends from 16 to 26 cm in radius; it provides r-ϕ points with a resolution of 150 μm. The 4.7 m long cylindrical TPC extends from 35 to 173.5 cm in radius. It provides up to 21 spatial points with a typical average precision of 173 μm in r-ϕ and 740 μm in z. The three tracking devices are immersed in a 1.5 Tesla magnetic field, parallel to the beam axis. For fully contained tracks, they yield a transverse momentum resolution $\sigma_{p_\perp}/p_\perp = 0.0006\, p_\perp \oplus 0.005$ ($p_\perp$ in GeV/c). For high-momentum tracks with VDET hits in both layers the impact parameter resolution can be parametrised as $\sigma_{d_0} = \sigma_{z_0} = 25 + 95/p$ (p in GeV/c, σ_{d_0} and σ_{z_0} in μm) in both r-ϕ and z coordinates.

The electromagnetic calorimeter (ECAL), placed inside the coil, is made of a barrel part and two endcaps and covers 98% of the solid angle. The readout of the lead/wire chamber layers is grouped in three stacks in depth, for a total thickness of $22X_0$, segmented in $0.9^\circ \times 0.9^\circ$ projective towers. The fine spatial granularity ensures excellent photon reconstruction. Assuming the neutral particles originate from the beam crossing point, the resolution of polar and azimuth angles are $\sigma_\theta/\sin\theta = \sigma_\phi = 0.25{+}2.5/\sqrt{E\,(\mathrm{GeV})}$ mrad. The energy resolution is $\sigma_E/E = 0.009 + 0.18/\sqrt{E\,(\mathrm{GeV})}$. The return yoke, instrumented with streamer tubes, acts as a hadron calorimeter (HCAL), 7 interaction lengths thick, which provides an energy measurement and a digital pattern of the energy deposition. It is surrounded by two layers of streamer muon chambers. The measurements of charged particle momenta from the tracking devices and of neutral energies from the calorimeters result in a typical resolution of 0.7 GeV on the hadron energy and 1.3 mrad on the hadron direction in τ decays.

Electrons are identified by the specific ionisation information measured in the TPC, by the consistency between the energy deposited in ECAL and the momentum measured by the tracking devices, and by the longitudinal and transverse shower profiles measured in ECAL. Muons are identified by the shower pattern in HCAL and a signal in the muon chambers. The resulting misidentification of leptons as hadrons is less than 0.6%, for a hadron identification efficiency of 98.3%.

3.2 Selection of hadronic τ decays

The lifetime analysis with the 3DIP method is performed on the ALEPH data collected from 1992 to 1994 at LEP, at centre-of-mass energies near the Z^0 peak ($\sqrt{s} \sim 91.25$ GeV). A sample of 105023 $Z^0 \to \tau^+\tau^-$ events is selected by using the standard ALEPH procedure described in [12] to which a few complementary cuts described in [13] are added to reduce the background contribution from non-τ sources to 0.8%. An overall efficiency, including geometrical acceptance, of 78.8% is measured from a sample of 1.06 million Monte Carlo events [14] going through the full detector simulation and selection procedure. The analysis is performed on real data and Monte Carlo generated data. The latter is used to estimate the biases in the method and adjust the results obtained from the data accordingly.

Due to the branching fractions of the hadronic channels, the events in which both τ's decay to hadrons are about 42% of the total sample. The analysis program designed for the branching ratio studies [15] is used to select that subsample and to improve the hadron energy measurement through an upgraded reconstruction of converted photons

and π^0 momenta. In order to reject interactions of the τ daughters with the detector material, the procedure also excludes the events with additional tracks having very large impact parameters ($|d_0| > 2\,\mathrm{cm}$ or $|z_0| > 10\,\mathrm{cm}$) or with hemispheres of even charge or unbalanced signs. Only events with 1-1 or 1-3 topologies are considered in the present lifetime analysis, at a loss of 4% due to events with higher charged multiplicities. Finally, the analysed data sample at peak amounts to 31833 events with a contamination from non-hadronic decays of less than 0.9%.

3.3 Quality cuts

As the 3DIP method uses both geometrical information (through $\delta\vec{C}_0$ and track angles) and kinematics (through $\vec{H}$), a rather severe selection is applied to ensure the quality of the hadron measurement, both in terms of spatial parameters and in terms of energy.

3.3.1 Quality cuts on tracking

The selection procedure demands that each hemisphere has at least one well measured track with momentum larger than 2 GeV/c, satisfying severe criteria on the vertex detector information, beyond the basic track quality requirements[1]:

- at least one r-ϕ hit and one z hit in the same VDET layer
- the above hits (r-ϕ and z) must not be shared with another track.

The latter requirement reduces considerably the track-hit misassociations occurring in three-prong decays, due to the small decay opening angle, or in one-prong decays, when the charged track overlaps with a pair from photon conversion.

Finally, a loose cut on the quality of the secondary vertex fit is applied to three-prong events, requiring the probability $\mathcal{P}(\chi^2_{\mathrm{vertex}})$ to be greater than 0.1%.

3.3.2 Quality cuts on $\vec{H}$ measurement

To keep the smearing term $(\ell^+\hat{\tau}^+ - \ell^-\hat{\tau}^-)\cdot\hat{H}$ small with respect to tracking errors, the tails of the orthogonality plot (Fig. 3) must be reduced. These tails are due to hadron mismeasurement or hard photon radiation in the initial or final state. Since there is no direct assessment of the orthogonality, an indirect quality selection is applied.

The selection makes use of the $\hat{\tau}\cdot\hat{H}$ orthogonality and the τ axis reconstruction from kinematics being both underlain by common physics presumptions: both rely on the absence of hard radiative emission and on the angles of each τ decay being well measured. The τ direction reconstruction, up to the twofold ambiguity, comes from the reduction of the cones, loci of each τ around the daughter hadron, to their intersections under the assumption that the τ's are back to back. It may happen however that the reconstructed two cones do not intersect; this is the signature that the physics hypotheses are not

[1] $|d_0| < 1.0$ cm, $|z_0| < 5.0$ cm; at least eight TPC hits and two ITC hits. Looser cuts are applied to the other two tracks of three-prong decays: $P > 0.1\,\mathrm{GeV/c}$, $|d_0| < 2.0$ cm, $|z_0| < 10.0$ cm; at least four TPC hits.

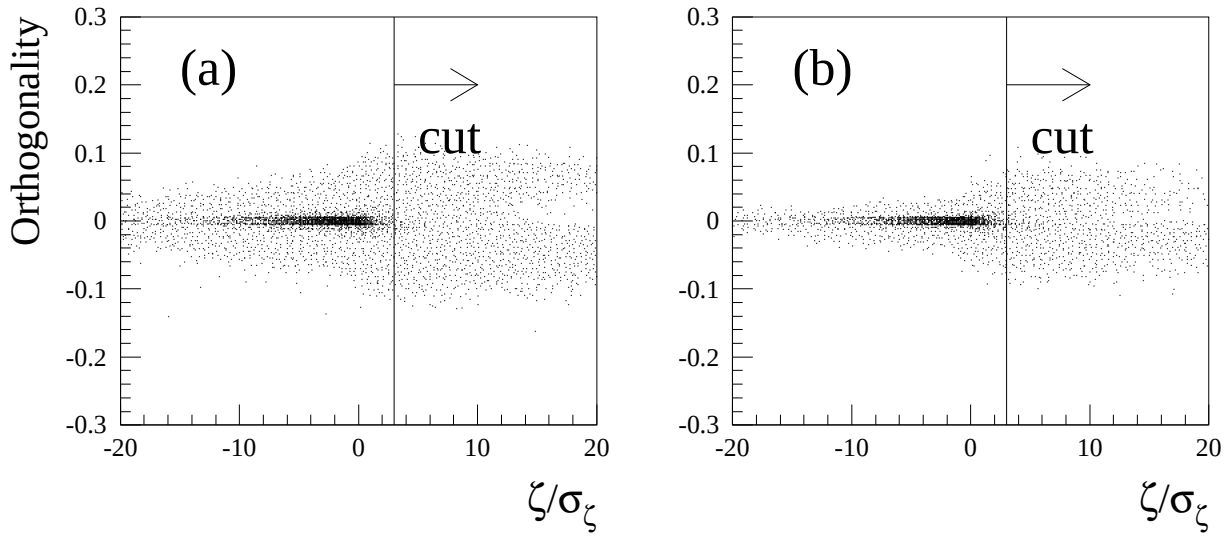

Figure 4: ζ/σ_ζ versus orthogonality $\hat{\tau}^{\pm} \cdot \hat{H}$; in Monte Carlo (a) 1-1 sample, (b) 1-3 sample. ζ measures the angular distance between the decay cones and is defined in the text. Each event enters the plot twice, with one entry per τ direction.

satisfied or that a large error is present in the hadron measurement due to π^0's or neutral hadrons escaping detection. The angular distance ζ between the two cones is defined from the acollinearity angle ξ between the two hadron directions and the τ decay angles $\psi^{\pm}$: $\zeta = 2\max(\xi, \psi^+, \psi^-) - (\xi + \psi^+ + \psi^-)$; its error σ_ζ is taken as $\sigma_\zeta^2 = \sigma_\xi^2 + \sigma_{\psi^+}^2 + \sigma_{\psi^-}^2$. There are two possible τ directions or none, depending on whether ζ is negative or positive, respectively. Events in which ζ is positive indeed coincide with events in which $\hat{\tau}^{\pm} \cdot \hat{H}$ is significantly different from zero, as seen in Fig. 4.

The cut $\zeta < 3\sigma_\zeta$ removes 12% of the 1-1 events and 16% of the 1-3 events. As the average decay angle is smaller in the three-prong decays than in the one-prong decays, the 1-3 configuration is expected to be more sensitive to the $\tau^+\tau^-$ acollinearity than the 1-1 configuration, as observed from the larger rate of rejected events in the 1-3 sample. After the cut is applied, the tails beyond 20 mrad in the orthogonality angle distribution are reduced from 14.2% to 6.4% of the final samples and the rms decreases from 35 mrad to 12.5 mrad (Fig. 5).

3.3.3 Additional cuts and summary

A few events with unphysically large impact parameters ($|\delta\vec{C}_0| > 2\,\mathrm{mm}$) or angles ($|\alpha^+ + \alpha^-| > 0.2$) are rejected. Only events with a reasonable confidence level enter the lifetime fit. A likelihood probability $\mathcal{P}(\mathcal{F})$ is defined as the integrated probability for an event to have a reconstructed δ equal to or larger than the observed value. $\mathcal{P}(\mathcal{F})$ is computed for a mean lifetime of 296 fs and events with a probability smaller than 10^{-3} are cut out.

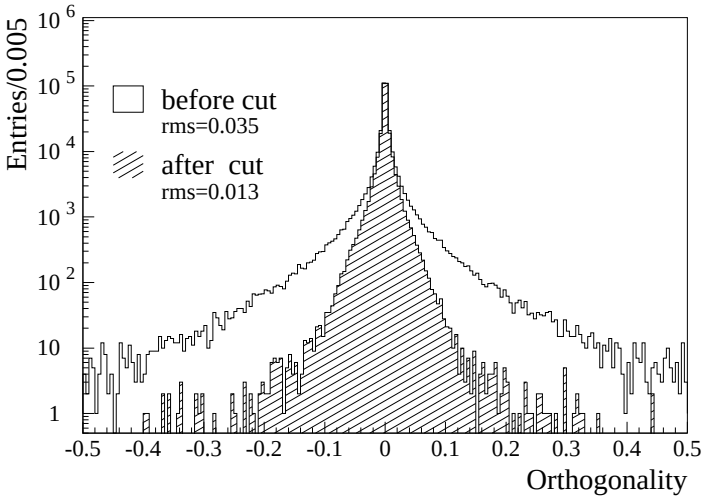

Figure 5: Orthogonality distributions before and after applying the $\zeta/\sigma_\zeta < 3$ cut in the Monte Carlo sample. Each event enters the plot twice, with one entry per τ direction.

Table 1 shows the number of events in each sample after the above cuts. The related systematic uncertainties are discussed in Sect. 5.

Table 1: Number of events in each sample at the peak energy after the quality cuts. Numbers in parentheses are efficiencies with respect to the previous line

	1-1 topology		1-3 topology	
	DATA	MC	DATA	MC
Number of hadronic $\tau^+\tau^-$	21170	167107	10663	84646
Track quality	13913(0.6572)	122833(0.7350)	7354(0.6897)	64893(0.7666)
$\mathrm{Prob}(\chi^2_{\mathrm{vertex}})$	-	-	5224(0.7104)	49347(0.7604)
$\zeta < 3\sigma_\zeta$	12264(0.8815)	108604(0.8842)	4394(0.8411)	41961(0.8503)
$\lvert\delta C_0\rvert < 2\,\mathrm{mm}$	12241(0.9981)	108373(0.9979)	4385(0.9980)	41878(0.9980)
$\lvert\alpha^+ + \alpha^-\rvert < 0.2$	12209(0.9974)	108024(0.9968)	4373(0.9973)	41771(0.9974)
$P(\mathcal{F}) > 10^{-3}$	12031(0.9854)	106508(0.9860)	4306(0.9847)	41267(0.9879)

4 Data analysis and results

4.1 Likelihood function

Ignoring radiative corrections to the τ momentum, the τ lifetime τ_τ converts to a mean decay length $\lambda = \gamma\beta c\tau_\tau$ with a boost factor $\gamma\beta = (E^2_{\mathrm{beam}}/m^2_\tau - 1)^{1/2}$. The distribution of the true 3DIP δ is the folding of two exponentials

$$\frac{dN}{d\delta^\pm} = \frac{1}{\lambda\alpha^\pm}\exp\left(-\frac{\delta^\pm}{\lambda\alpha^\pm}\right) \tag{6}$$

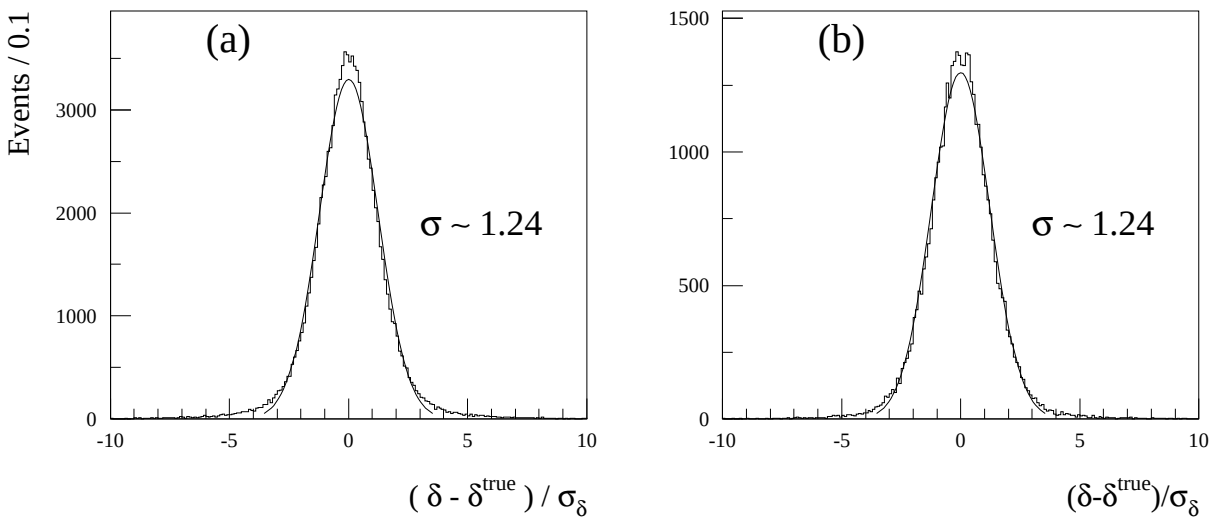

Figure 6: Pull distribution $(\delta - \delta^{\rm true})/\sigma_\delta^{\rm Tracking}$ in Monte Carlo (a) 1-1 sample (b) 1-3 sample. δ is the reconstructed 3DIP; $\delta^{\rm true}$ is defined as $\delta\vec{C}_0^{\rm true} \cdot \hat{H}$, where $\delta\vec{C}_0^{\rm true}$ is computed at generation level and $\hat{H}$ is the reconstructed projection direction.

with the constraint that the two $\delta^\pm \equiv (\vec{T}_0 - \vec{C}_0^\pm) \cdot \vec{H}$ sum up to δ [8]. The expected distribution for the observed 3DIP δ is derived by convolving the true distribution Eq. (6) with the experimental error functions. The resolution function is well approximated by a Gaussian distribution (Fig. 6). A small contribution ($\sim$6 μm on average) comes from the transverse size of the luminous region ($\sigma_x^{\rm beam}\sim$110 μm in 1992, 160 μm in 1993 and 125 μm in 1994; $\sigma_y^{\rm beam}\sim$5 μm). It is interesting to note that the large spread of the beam crossing region along the z-axis ($\sim$7 mm) does not affect any of the components of the $\delta\vec{C}_0$ measurement.

As already shown in Sect. 2.2, the measurement of $\alpha^\pm$ is not affected by the undetected neutrinos in τ decay and tracking errors are small enough ($\sim$0.5 mrad) to be neglected. The likelihood function $\mathcal{F}$ for a given mean decay length λ is therefore the convolution of the true δ distribution with a single Gaussian resolution function, of width $\sigma = \sigma_\delta$:

$$\mathcal{F}(\delta, \alpha^+, \alpha^-, \sigma; \lambda) = \frac{1}{2\lambda(\alpha^+ - \alpha^-)} \exp\left(-\frac{\delta^2}{2\sigma^2}\right) \left(s_+ \exp Q_+^2 \,\mathrm{erfc}\, Q_+ - s_- \exp Q_-^2 \,\mathrm{erfc}\, Q_-\right)$$

where $Q_\pm = \dfrac{s_\pm}{\sqrt{2}}\left(\dfrac{\sigma}{\lambda\alpha^\pm} - \dfrac{\delta}{\sigma}\right)$, $s_\pm$ are the signs of $\alpha^\pm$ and erfc is the complementary error function.

Although the tracking resolution function is well described by a Gaussian distribution, a calibration of errors is needed, on real as well as on simulated data, due to the imperfect modelling of the tracking errors in the helix fit.

In previous impact parameter analyses [1, 3, 4], the d_0 resolution was calibrated using Monte Carlo and reference data samples like dimuon events or $Z^0 \to q\bar{q}$ events. In

the present approach, the calibration is performed on the analysed data themselves. The uncertainty on δ due to tracking errors is scaled by a global factor κ: $\sigma_\delta = \kappa\sigma_\delta^{\mathrm{Tracking}} \oplus \sigma_\delta^{\mathrm{BP}}$, which is fitted simultaneously with the mean lifetime τ_τ in a two-parameter maximum likelihood fit. The validity of this procedure is directly related to the fact that, in contrast to the IPS method, no angular error affects the δ-to-$\alpha^\pm$ relationship (Eq. (4)). The robustness of the two-parameter fit and the implications on the systematic errors are addressed in detail in the following sections.

4.2 Orthogonality Correction

Equation (4) is established under the assumptions that the τ's are back to back and the final hadrons are measured with no error, so that $\hat{\tau} \cdot \hat{H}$ vanishes. In presence of radiative emission and/or detector-induced distortions, the exact equation[2] obtained when projecting Eq. (3) to $\hat{H}$ is

$$\delta = \ell^+(\alpha^+ - \hat{\tau}^+ \cdot \hat{H}) + \ell^-(\alpha^- - (-\hat{\tau}^- \cdot \hat{H}))$$

In that equation, the orthogonality terms $\pm\hat{\tau}^\pm \cdot \hat{H}$ appear as corrections on the measured angles $\alpha^\pm$. Although much smaller on average than α ($\sim$7%) and symmetrically distributed about zero, orthogonality is not equivalent to a random angular fluctuation. When the size of $\hat{\tau} \cdot \hat{H}$ exceeds the τ decay opening angle, *i.e.*, the angle between the τ and the charged track, the sign of $\hat{\tau} \cdot \hat{H}$ is indeed correlated with the sign of $\hat{c} \cdot \hat{H}$, hence with the sign of α ($\alpha^\pm \equiv \pm\hat{c}^\pm \cdot \hat{H}$). As a consequence, when the correction is ignored in the likelihood function, the tails of the orthogonality distribution induce a systematic underestimation of the τ lifetime of a few percent.

To correct for that intrinsic bias, the lifetime result obtained from the data could be shifted *a posteriori* by the same amount as observed in Monte Carlo. The alternative, event-by-event procedure used in the present analysis minimises the bias *a priori*, by correcting the measured angles $\alpha^\pm$ by the average orthogonality $\langle \pm\hat{\tau}^\pm \cdot \hat{H} \rangle (\alpha^\pm)$, as a function of $\alpha^\pm$ themselves. The correction as observed in Monte Carlo (Fig. 7) is applied both to real and simulated data. Because the average opening angle, hence α, is smaller in the 3-prong decays than in the one-prong decays, the relative correction is larger on the 3-prong side. The correction is drastically reduced at large α by the orthogonality cut (Sect. 3.3.2).

4.3 Results

The analysis has been performed on 1992, 1993 and 1994 data independently, and for each LEP centre-of-mass energy. All mean lifetime results agree within statistical errors, and in the following the combined results from the data taken at the peak energy are presented.

[2]The equality holds for any projecting direction, in the $\epsilon^\pm \simeq \ell^\pm$ approximation (Sect. 2.2).

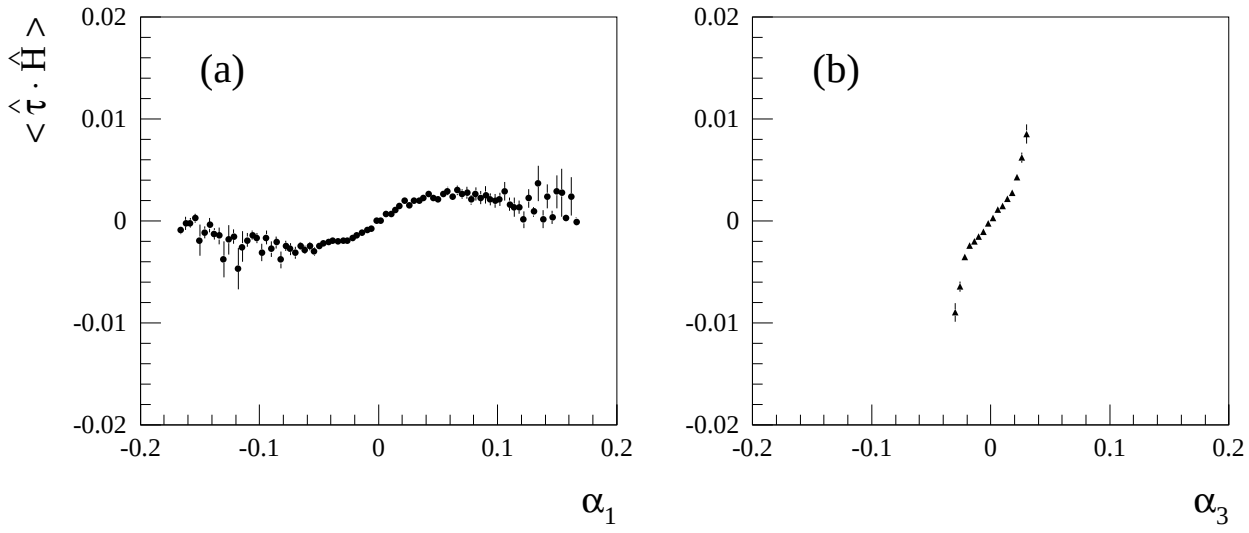

Figure 7: Correlation between the average orthogonality $\langle \pm\hat{\tau^{\pm}} \cdot \hat{H} \rangle$ and the $\alpha^{\pm}$ angles in the 1-3 Monte Carlo sample; (a) on the one-prong side, (b) on the three-prong side. Correlations observed in the 1-1 sample are similar to figure (a)

4.3.1 Results of the analysis of the 1-1 and 1-3 samples

The results of the two-parameter likelihood maximisation are summarised in Table 2 from the 1-1 sample and the 1-3 sample.

Table 2: The fitted lifetimes and error calibration factors from the 1-1 and 1-3 samples. The assumed lifetime in Monte Carlo generation is 296 fs.

		Data	Monte Carlo
1-1 sample	τ_τ (fs)	286.94 ± 3.05	294.87 ± 1.03
	κ	1.3091 ± 0.0177	1.2470 ± 0.0058
1-3 sample	τ_τ (fs)	291.10 ± 5.59	294.26 ± 1.82
	κ	1.3189 ± 0.0254	1.2353 ± 0.0080

The lifetime values fitted on Monte Carlo are within statistical errors of the expected value. Residual biases of $-0.38 \pm 0.35\%$ ($-0.59 \pm 0.62\%$), are calculated in the 1-1 (1-3) analyses. After the results obtained in the data are adjusted accordingly, the lifetimes measured in the 1-1 and 1-3 data samples are $288.0 \pm 3.1 \pm 1.0$ (MC stat) fs and $292.8 \pm 5.6 \pm 1.8$ (MC stat) fs, respectively.

The fitted values of the κ parameter in Monte Carlo are consistent with the resolution distributions (Fig. 6). Differences of $(5.0 \pm 1.5)\%$ in the 1-1 sample and $(6.8 \pm 2.2)\%$ in the 1-3 sample are observed between the resolution scale factors fitted on data and

Monte Carlo. This comes from residual alignment errors in data, imperfect modelling of physical processes (nuclear interactions, multiple scattering) and detector (amount of traversed material, VDET efficiency) in Monte Carlo. However, because of the small correlation between τ_τ and κ (see next section), no bias is induced on the lifetime fit by these differences; the self-adjustment of the error calibration prevents the lifetime fit from being sensitive to the resolution uncertainties, as discussed in the next section and Sect. 5.

4.3.2 τ_τ - κ decoupling

Weak correlations of -26.3% (-25.4%) between the errors on τ_τ and κ are measured in the fits over the 1-1 (1-3) samples. The analysis of the likelihood function reveals that τ_τ and κ are determined by two distinct classes of events. This is illustrated by Fig. 8, which shows the distribution of the second derivatives of the likelihood function $\mathcal{F}(\delta, \alpha^+, \alpha^-, \sigma; \lambda, \kappa)$ with respect to λ and κ. Only the events with a small likelihood probability ($\mathcal{P}(\mathcal{F}) < 0.2$) enter the plot; the events with larger $\mathcal{P}(\mathcal{F})$ show the same pattern as Fig. 8 but both second derivatives are smaller and consequently the events have smaller weight in the maximum likelihood determination. The sample clearly subdivides into two groups, Group A and Group B in the figure, yielding complementary sensitivities to λ and κ. The first class (large negative $\partial^2\mathcal{F}/\partial\lambda^2$ and $\partial^2\mathcal{F}/\partial\kappa^2 \sim 0$) has a large weight in the λ fit, but none in the κ fit. They are events with long decay lengths with an exponential $|\delta|$ distribution (Fig. 8.b,c). The second class (large negative $\partial^2\mathcal{F}/\partial\kappa^2$ and $\partial^2\mathcal{F}/\partial\lambda^2 \sim 0$) has a large weight in the κ fit but none in the λ fit. The δ distribution is Gaussian around zero (Fig. 8.b,d). They are "unphysical" events in which the measured values of δ and $\alpha^\pm$ are incompatible with positive τ decay lengths, but for resolution effects. As there is no contribution from angular uncertainties, the δ distribution of these "unphysical" events gives a direct constraint on the tracking resolution.

5 Systematic uncertainties and checks

5.1 Selection-induced systematic errors

In order to estimate the effects of the selection procedure on the lifetime measurement, the cuts are either switched on/off or varied and an estimate of the error is inferred from the maximum variation of the results. The main contribution comes from the vertex probability cut applied to the three-prong decays which is responsible for a 0.61% uncertainty in the 1-3 analysis. Residual non-τ backgrounds or residual leptonic τ decays give negligible contributions ($< 0.05\%$) to the systematic errors. The uncertainty associated with the residual contamination of the 1-3 sample by τ decays involving K^0_S, with $K^0_S \to \pi^+\pi^-$, is estimated by Monte Carlo simulation allowing for the branching ratios of those channels to vary within their errors; the effect is negligible ($< 0.02\%$).

5.2 Uncertainty on the orthogonality correction

Since the bias due to nonzero $\hat{\tau} \cdot \hat{H}$ is corrected by means of the Monte Carlo, discrepancies between data and Monte Carlo might induce a systematic shift of the lifetime

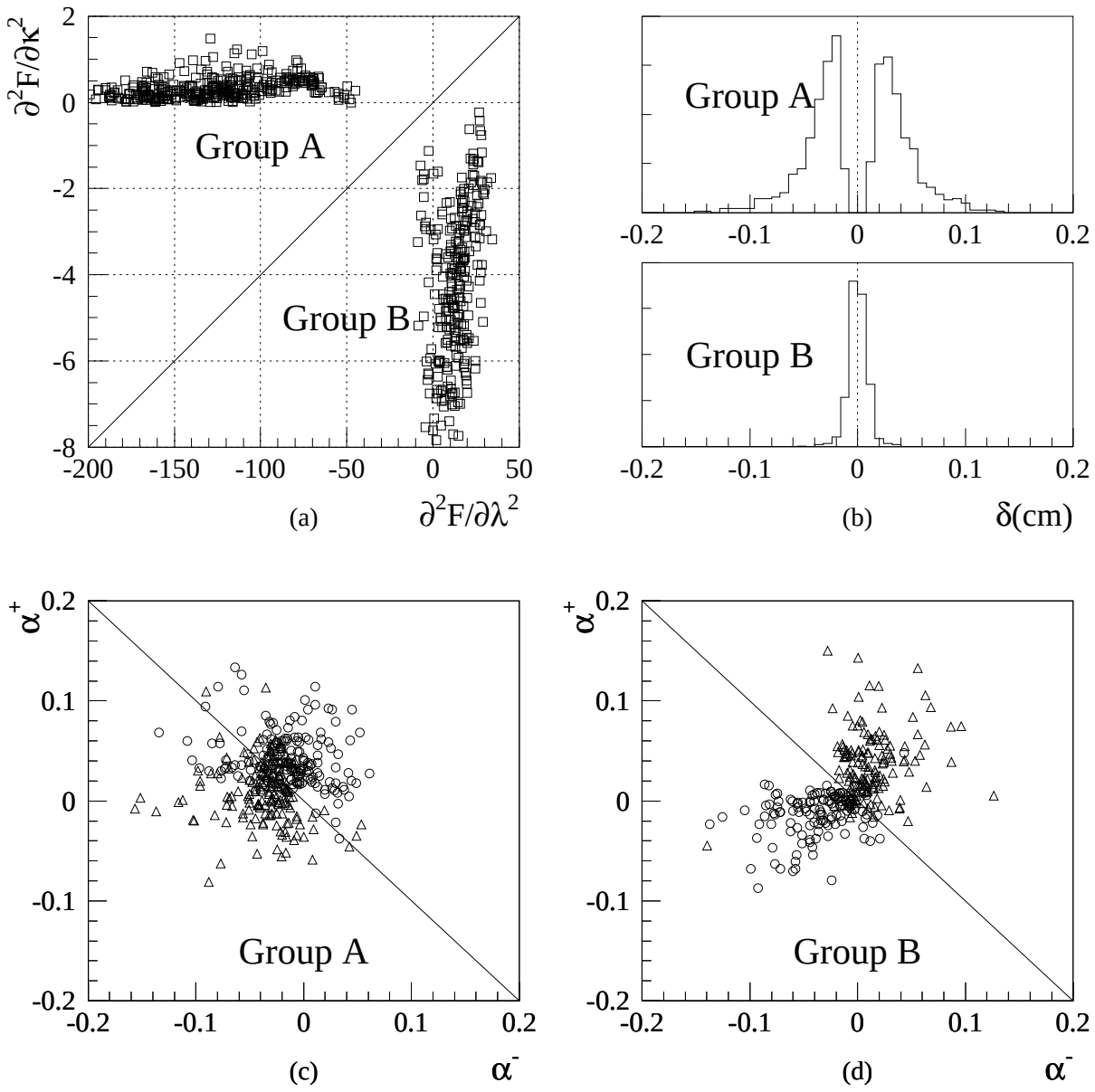

Figure 8: (a) $\partial^2\mathcal{F}/\partial\lambda^2$ versus $\partial^2\mathcal{F}/\partial\kappa^2$ for a 1-1 data subsample (see text); (b) δ distributions for each group. Group A features a bipolar exponential distribution; group B shows the Gaussian distribution expected from experimental resolution; (c) α^+ versus α^- for group A (d) α^+ versus α^- for group B. Events with positive δ are plotted as circles, events with negative δ are plotted as triangles. For group B events, the sign of δ is inconsistent with the signs of $\alpha^\pm$ for positive decay lengths.

measurement. Uncertainties on the $\hat{\tau} \cdot \hat{H}$ orthogonality depend on the accuracy of the simulation of the $e^+e^- \to \tau^+\tau^-$ process, the τ decay (radiative corrections, τ polarisation, branching fractions of poorly measured hadronic channels, *e.g.*, involving K^0_L) and the detector response (photon reconstruction efficiency, lepton identification). As there is no direct test of the orthogonality, the related systematic uncertainty is estimated on the basis of measured quantities correlated to $\hat{\tau} \cdot \hat{H}$, *e.g.*, the distributions of $\alpha^{\pm}$ themselves or the angular distance ζ between the decay cones. Data and Monte Carlo distributions of relevant quantities are compared with the quality cut on orthogonality (ζ/σ_ζ cut) removed in order to include the effect of that cut. The data to Monte Carlo ratios of the fractions of events in the tails, of the average values or rms are checked for deviations from unity and slopes with respect to α. No deviation from unity exceeding 2% (5%) is observed in the 1-1 (1-3) samples, including statistical fluctuations; slopes are consistent with zero within statistical errors. When accounting for such uncertainties on the average $\hat{\tau} \cdot \hat{H}$ correction applied in the data, the fitted lifetime remains stable within 0.14% (0.40%) in the 1-1 (1-3) sample. The resolution factor κ is left unchanged.

5.3 Uncertainties of alignment corrections and resolution function

Detector misalignments cause systematic offsets in d_0 and z_0 impact parameter measurements in real data. In 3DIP as in other IPS-like methods, the effect is however largely cancelled due to the angular symmetries of the τ pair event distribution. The offsets have been mapped as function of θ and ϕ, using the impact parameters measured in $e^+e^- \to q\bar{q}$ events with respect to the primary vertex. The lifetime is calculated after the measured offsets are subtracted. The effect of the correction is 0.25% (0.35%) in the 1-1 (1-3) sample, dominantly from the d_0 offsets. The systematic error related to detector misalignments is estimated from the observed changes when the offset correction is fluctuated within its errors. Systematic uncertainties of 0.08% and 0.27% are assigned for alignment errors on the lifetime, in the 1-1 and 1-3 samples, respectively. The fitted value of the resolution factor κ is minimal for the nominal values of the offset correction and increases by up to 2.5% when the correction is not applied.

Several checks have been made to investigate the stability of the lifetime measurement against the uncertainties of the resolution function, which are the major source of systematic errors in some methods.

The dependence of the lifetime fit on the parametrisation of the resolution function has been studied. The multiplicative κ scheme has been changed to an additive ρ scheme, $\sigma_\delta = \sigma_\delta^{\mathrm{Tracking}} \oplus \sigma_\delta^{\mathrm{BP}} \oplus \rho$; the results of the fits show no more than 0.14% change in τ_τ with respect to the multiplicative scheme, with a fitted ρ term of $35 \pm 1\,\mu$m. The three-prong error calibration κ_3 has been allowed to be 10% larger than the one-prong κ_1 factor. When such a difference is assumed in the likelihood fit of the 1-3 sample, the lifetime result changes less than 0.20%. The lifetime fit is also stable when one allows for different κ factors for d_0 and z_0: a 0.06% shift of the lifetime is observed when a 6% difference between transverse and longitudinal error calibrations is assumed, as observed in resolution studies on Monte Carlo.

The stability of the measured lifetime has been checked with respect to an artificial

degradation of the δ resolution. Most of the effect of the additional error is borne by the κ factor which grows by 4% when the resolution degrades by 5%, while the τ_τ fitted value remains constant within less than 0.3%. Conversely, were the difference in κ fitted in Monte Carlo and data to be interpreted as an uncertainty on the resolution measurement, the lifetime would not be affected by more than 0.3%. As a further check of uncertainties related to the VDET track selection and material modelling, the fitted lifetime has been studied as a function of the τ polar angle; no effect larger than the expected statistical fluctuation has been observed.

Special care has been given to the effect of non-Gaussian tails of the resolution function. Since they are not considered in the likelihood function, these contributions could cause a bias in the lifetime fit. A discrepancy in the population of tails in real data compared to Monte Carlo might then induce a systematic error. Non-Gaussian tails beyond $2\sigma_\delta$ amount to 6.7% of the 1-1 Monte Carlo sample and 7.3% of the 1-3 sample. From resolution studies on real and Monte Carlo $q\bar{q}$ events [4], it is assessed that the simulation of the tails is accurate to 20%. The uncertainty on the non-Gaussian population has different consequences whether it affects the far tails ($|\delta - \delta^{\rm true}| > 3\sigma_\delta$) or the near tails ($2\sigma_\delta < |\delta - \delta^{\rm true}| < 3\sigma_\delta$). The uncertainty of the near tails is totally absorbed by the fitted calibration factor κ and the lifetime is left unchanged ($< 0.1\%$ variation) in any sample. When the Monte Carlo far tails are varied to account for the uncertainty (20%), the κ factor, which measures the core of the resolution function, is hardly affected. The maximum variations of the fitted lifetime are nevertheless not larger than 0.25% in both samples.

As the distributions of the resolution function are similar for muons and hadrons, but for far tails [4], a check of the resolution fitted on real data is provided by the $Z^0 \to \mu^+\mu^-$ events. A sample of these "zero-lifetime" events has passed through the same selection and analysis programs as the $Z^0 \to \tau^+\tau^-$ events, apart from the by-passed hadron selection. The fitted scaling factor $\kappa^{Z^0\to\mu^+\mu^-} = 1.258 \pm 0.006$ is in excellent agreement with the width (1.248 ± 0.010) of the δ/σ_δ distribution of those events, which measures the resolution calibration.

5.4 Summary of systematic errors

The above intrinsic uncertainties sum up to 0.3% in the 1-1 analysis and 0.8% in 1-3 analysis. They are summarised in Table 3, which also includes the Monte Carlo statistical errors. The quoted total uncertainty assumes no correlations between the systematic sources.

The stability of the lifetime measurement results from the fact that the two parameters in the simultaneous fitting procedure are decoupled. Most of the effects on the lifetime fit related to tracking uncertainties (resolution, alignment, vertex fit efficiency) are damped by the self-calibration of the κ factor.

Table 3: Summary of systematic errors in fs.

Sources	1-1	1-3
Monte Carlo statistics	1.03	1.82
Data selection	0.12	0.11
Cut on vertex χ^2	-	1.77
Orthogonality cut and correction	0.41	1.13
Resolution function uncertainties	0.75	0.78
Detector misalignment	0.23	0.78
Total	1.35	3.00

6 Correlations with other methods

The hadronic τ decay events form subsamples of the samples used in the other methods: the 1-1 events in the IPS-like or IPD analyses; the 1-3 events in the DL analysis. Some statistical correlations between the present method and the others are therefore expected. The correlations are computed by splitting the Monte Carlo samples into a number of subsamples and fitting the lifetime separately by the different methods.

Since the d_0 sum enters the δ definition (see the approximate expansion in Eq. (5)), a correlation is expected between the present 1-1 analysis and IPS-like methods. It is however damped by the projection to $\vec{H}$ and the z_0 difference contribution. The correlation factor is found to be 0.64 ± 0.06 for events in which both τ's decay to hadrons. The net correlation with IPS-like results is however much smaller (0.30 ± 0.06) since the latter samples include leptonic decays. The net correlation with the IPD result is found to be 0.24 ± 0.06.

Even when the 1-3 analysis and DL are performed on the same τ pair samples, a weak correlation is expected between the 3DIP and DL methods since the latter uses only the three-prong side of the event. Furthermore, for given decay lengths $\ell^{\pm}$, the smaller the τ decay angle, the smaller the contribution to the 3DIP impact parameter δ, and therefore the smaller the weight on the lifetime fit. As the one-prong τ decay angles tend to be larger than the three-prong ones, the result of the 3DIP 1-3 analysis is consequently driven by the one-prong side of the events. A statistical correlation smaller than 0.17 is obtained between the DL and the 3DIP methods applied to the same samples. The net correlation is 0.06 ± 0.05.

7 Conclusions

A new method has been developed to measure the τ lepton lifetime in the $Z^0 \to \tau^+\tau^-$ events when both τ's decay to hadronic modes. The method is an impact parameter sum generalised to three-dimensional space. As such, it is free from the uncertainties on the τ production point due to the beam size. The special projection of the decay-track miss distance along an axis normal to the τ direction, precisely defined from kinematics only, makes the method free from the uncertainties on the τ direction as well. The resulting negligible angular smearing allows the experimental resolution to be fitted together with

the decay length, in a two-parameter likelihood procedure. The method is therefore self-consistent and self-calibrating, independent from the resolution studies based on external reference samples. A bias of a few percent arises from the projecting direction not being strictly normal to the τ direction, due to hadron mismeasurement or radiative effects. It is corrected by means of a Monte Carlo simulation, with a related systematic error estimated below 1 fs.

The results from the 3DIP method for 1-1 and 1-3 samples using the 1992–1994 ALEPH data are

$$\tau_\tau^{1-1} = 288.0 \pm 3.1 \pm 1.3\,\mathrm{fs}$$
$$\tau_\tau^{1-3} = 292.8 \pm 5.6 \pm 3.0\,\mathrm{fs},$$

respectively.

The two measurements agree within their errors. The combined result of 1-1 and 1-3 analyses is

$$\tau_\tau = 289.0 \pm 2.7 \pm 1.3\,\mathrm{fs}.$$

Due to the restricted sample to which the method applies, and the choice of stringent cuts made for the present analysis, especially on the track quality in the vertex detector, the overall acceptance is about 12% with respect to the total number of τ pair events produced. However, the reduced statistics is somewhat compensated by the high sensitivity achieved, $1.2/\sqrt{N_{\tau\tau}}$ (with $N_{\tau\tau}$ the number of selected τ pairs).

The 3DIP method uses information that is ignored in the other analyses: the z_0 component of the impact parameter, and full detector information for the kinematical reconstruction of the τ decays. As a result, the 3DIP measurement is weakly correlated with the other methods. The present results from 1992–1994 data are combined with the previously published ALEPH measurements [4], taking into account the statistical and systematic correlations. The combined result of the τ lepton lifetime is

$$\tau_\tau = 291.2 \pm 2.0 \pm 1.2\,\mathrm{fs}$$

with a χ^2 of 8.1 for 12 degrees of freedom. It is consistent with the most recent measurements by other collaborations [16, 17, 18, 19, 20].

8 Acknowledgements

We wish to thank our colleagues in the CERN accelerator divisions for the successful operation of LEP. We are indebted to the engineers and technicians in our all institutions for their contributions to the excellent performance of ALEPH. Those of us from non-member countries thank CERN for its hospitality.

References

[1] *"Lifetime measurement techniques"*, Proceedings of the Third Workshop on Tau Lepton Physics, L. Rolandi editor, Nucl. Phys. B (Proc. Suppl.) 40 (1995) 295

[2] D. Decamp et al. (ALEPH Collaboration), Phys. Lett. B 279 (1992) 411

[3] D. Buskulic et al. (ALEPH Collaboration), Phys. Lett. B 297 (1992) 432

[4] D. Buskulic et al. (ALEPH Collaboration), Z. Phys. C 70 (1996) 549

[5] P. Abreu et al. (DELPHI Collaboration), Phys. Lett. B 302 (1993) 356

[6] R.M. Barnett et al., Particle Data Group, Phys. Rev. D 54 (1996) 256, and references herein

[7] Y.S. Tsai and A.C. Hearn, Phys. Rev. B 140 (1965) 721

[8] I. C. Park, Ph.D. thesis, LAL 95-03, February 1995

[9] D. Decamp et al. (ALEPH Collaboration), Nucl. Inst. & Meth. A 294 (1990) 121

[10] D. Buskulic et al. (ALEPH Collaboration), Nucl. Inst. & Meth. A 360 (1995) 481

[11] G. Batignani et al, conference record of the 1991 IEEE Nuclear Science Symposium (November 1991, Sante Fe, NM, USA), Vol. 1, p. 438; B. Mours et al, Nucl.Instrum.Meth.A379 (1996) 101

[12] D. Buskulic et al. (ALEPH Collaboration), Z. Phys. C 62 (1994) 539

[13] D. Buskulic et al. (ALEPH Collaboration), Z. Phys. C 70 (1996) 561

[14] Computer program KORALZ, version 3.8, courtesy of S. Jadach, B.F.L. Ward and Z. Was ; S. Jadach and Z. Was, Comp. Phys. Comm. 36 (1985) 191 ; S. Jadach, B.F.L. Ward and Z. Was, Comp. Phys. Comm. 66 (1991) 276

[15] D. Buskulic et al. (ALEPH Collaboration), Z. Phys. C 70 (1996) 579

[16] K. Abe et al. (SLD Collaboration), Phys. Rev. D 52 (1995) 4828

[17] P. Abreu et al. (DELPHI Collaboration), Phys. Lett. B 365 (1996) 448

[18] G. Alexander et al. (OPAL Collaboration), Phys. Lett. B 374 (1996) 341

[19] R. Balest et al. (CLEO Collaboration), Phys. Lett. B 388 (1996) 402

[20] M. Acciarri et al. (L3 Collaboration), CERN-PPE-96-124, Sep 1996, submitted to Phys. Lett. B